J Comp Physiol A (2000) 186: 467–479

ORIGINAL PAPER

R. Kern · M. Lutterklas · M. Egelhaaf

Neuronal representation of optic flow experienced by unilaterally blinded flies on their mean walking trajectories

Accepted: 29 February 2000

Abstract Asymmetries in the optic flow on both eyes may indicate an unintended turn of an animal and evoke compensatory optomotor responses. On a straight path in an evenly structured environment, the optic flow on both eyes is balanced corresponding to a state of optomotor equilibrium. When one eye is occluded an optomotor equilibrium is expected to be reached on a curved path provided that the translatory optic flow component is cancelled by a superimposed rotation. This hypothesis is tested by analysing how the HSE cell, a constituent element of the fly's optomotor system, represents optic flow in behavioural situations. The optic flow as seen on the average trajectory of freely walking monocular flies is reconstructed. This optic flow is used as stimulus of the HSE cell in electrophysiological experiments and as input of a model of the fly's optomotor system. The responses of the HSE cell and of the model fluctuate around the resting potential. On average, they are much smaller than the responses evoked by optic flow experienced on a straight path. These results corroborate the hypothesis that the mean trajectory of monocular flies corresponds to a path of optomotor equilibrium.

Key words Vision · Optic flow · Optomotor behaviour · Course control · Fly

Abbreviations *HS* horizontal system · *T* trajectory

Introduction

Walking behaviour of flies is not affected dramatically by occluding one of the eyes. It is hardly possible to infer from observing walking flies whether they have only one or both eyes at their disposal to collect information about their visual surround and about the direction and speed of self-motion. Nonetheless, the average trajectory of monocular flies bends towards the open eye, whereas binocular animals, on average, walk straight (Kern and Egelhaaf 2000). The following hypothesis might explain this behavioural finding. It is assumed that the optic flow in front of the two eyes is compared somewhere in the nervous system, in order to infer whether the animal is moving on a straight or a curved path. Accordingly, a balanced optic flow is interpreted to represent a state of optomotor equilibrium which indicates straight locomotion. If the translatory motion is superimposed by rotations about the animal's vertical axis, the overall optic flow in the visual field of one eye differs from that of the other eye. This imbalance may induce compensatory turns, if an animal with both eyes intact intends to move straight rather than along a curved course. On the basis of this concept (Götz 1975) it has been postulated (Kern and Egelhaaf 2000) that in an animal with one eye occluded an optomotor equilibrium can only be achieved on a path bent towards the open eye. The optic flow induced by the translational component of locomotion is then assumed to be cancelled by the optic flow induced by the superimposed rotation. To test this hypothesis we analyse how the brain represents optic flow on the assumed path of optomotor equilibrium of monocular flies. Since it is not possible for technical reasons to record neuronal activity whilst the fly moves around, we videotaped flies walking freely in known environments (Fig. 1A) and subsequently reconstructed the world as seen out of the fly's eye during walking (Fig. 1B–D). The behaviourally generated optic flow is used for visual stimulation in electrophysiological experiments where the response of a representative neuron in the fly's optomotor system, the HSE cell, is analysed (Fig. 1E). In addition, the stimuli are used as input to a model of the fly's motion pathway which is based on experimentally established circuits of the optomotor system (Fig. 1F, Fig. 2).

R. Kern (✉) · M. Lutterklas · M. Egelhaaf
Lehrstuhl für Neurobiologie, Fakultät für Biologie,
Universität Bielefeld, Postfach 10 01 31,
D-33501 Bielefeld, Germany
e-mail: roland.kern@biologie.uni-bielefeld.de
Fax: +49-521-106-6038

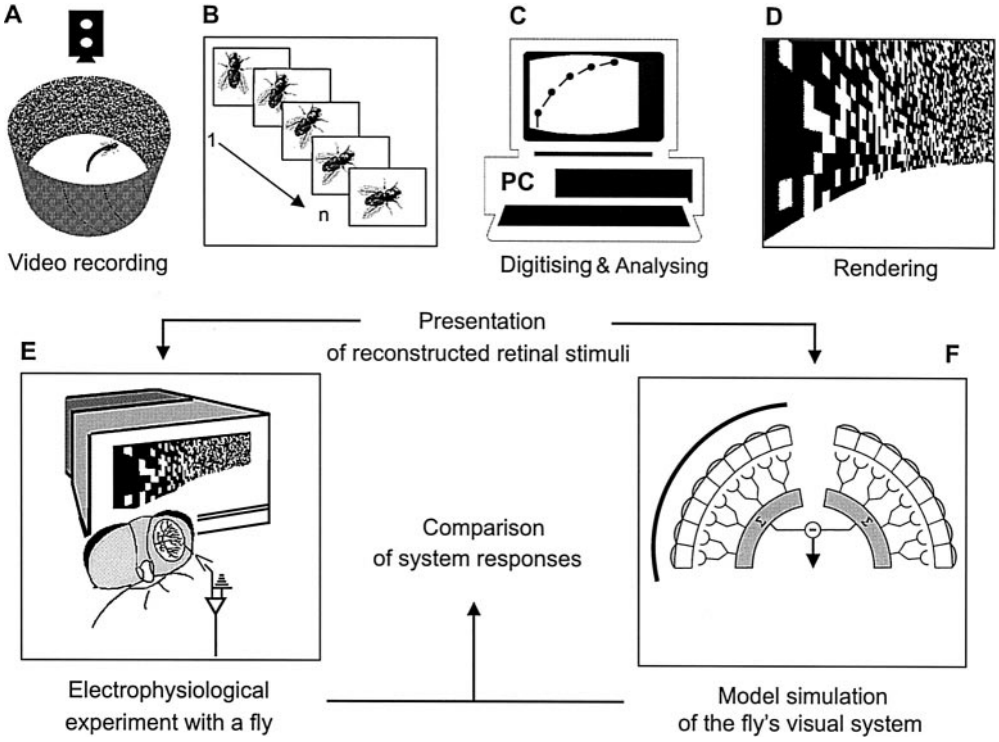

Fig. 1A–F Approach used in the present study. Flies walking freely in an arena are video recorded (**A**). The video is grabbed off-line frame by frame (**B**). The position and orientation of the fly is determined in each digitised video frame and used to calculate the trajectory of the animal (**C**). The trajectory data are used to control the path of a simulated camera in a virtual 3D environment that mimics the original arena. Pictures are taken by the camera at time intervals of 10 ms (**D**). The size of the camera's field of view as well as the azimuth and the elevation of the camera's central axis are adjusted to cover large parts of the receptive field of the HSE cell in the fly optomotor system. The HSE cell is stimulated in subsequent electrophysiological experiments by the sequence of images reconstructed in this way (**E**). The same images are fed into a model of the fly's optomotor system (**F**, details shown in Fig. 2). The local motion computations as well as the integration (**Σ**) of the local motion signals are indicated schematically for the left and right part of the model visual system. Stimuli are presented to only the right eye of the fly and of the model visual system. The output of the real visual system and the model system are compared to each other

There is evidence that the so-called horizontal system (HS) cells in the fly's motion pathway (Hausen 1982a, b) play a prominent role in optomotor course control. This evidence is provided by the similarity of the response characteristics of the cells and optomotor turning responses of tethered flies flying in a flight simulator (reviews: Egelhaaf and Borst 1993a; Egelhaaf et al. 1988; Hausen 1981), and from behavioural experiments on flies without these cells due to either microsurgery (Geiger and Nässel 1981; Hausen and Wehrhahn 1983, 1990) or mutation (Heisenberg et al. 1978). The HS cells spatially pool with their extended dendrites the outputs of many retinotopically arranged local motion sensitive elements. As a consequence, the response of the HS cells is directionally selective to horizontal motion in large parts of the visual field. They depolarise during front-to-back motion and hyperpolarize during back-to-front motion in the ipsilateral visual field (Hausen 1982a, b). The graded depolarizations may be accompanied by spike-like events. There are three HS cells in each half of the visual system which have their receptive fields in the dorsal (HSN), the medial (HSE) and the ventral (HSS) part of the visual field, respectively. The HS cells are not equally sensitive to motion in their entire receptive fields. Rather, their sensitivity varies along both the azimuth and the elevation. Along the azimuth, the sensitivity is maximal in the fronto-lateral part of the visual field (Hausen 1982b). The HS cells do not summate their retinotopic inputs linearly: the HS cell responses first increase with the number of activated inputs and then reach a more or less constant plateau level. Nonetheless, the response amplitude still depends on the velocity of stimulus motion (Hausen 1982b). Hence, the plateau level is not a result of output saturation of the HS cells, but rather of a gain control mechanism (Hausen 1982b; Egelhaaf and Borst 1993b; Borst et al. 1995; Single et al. 1997). There are two types of retinotopic input elements of the HS cells with opposite polarity which inhibit and excite the cell, respectively. The HS cells do not represent unambiguously the stimulus motion in the respective patch of the visual field according to its direction and velocity. Rather, the signals also depend on the textural properties of the stimulus, such as its spatial frequency content and contrast (review: Egelhaaf and Borst 1993b). Moreover, the HS cells represent the time-course of stimulus velocity only within a limited dynamic range (Egelhaaf and Reichardt 1987; Haag and Borst 1998). It was proposed that the difference between the responses of HS cells in the left and right half of the brain signals

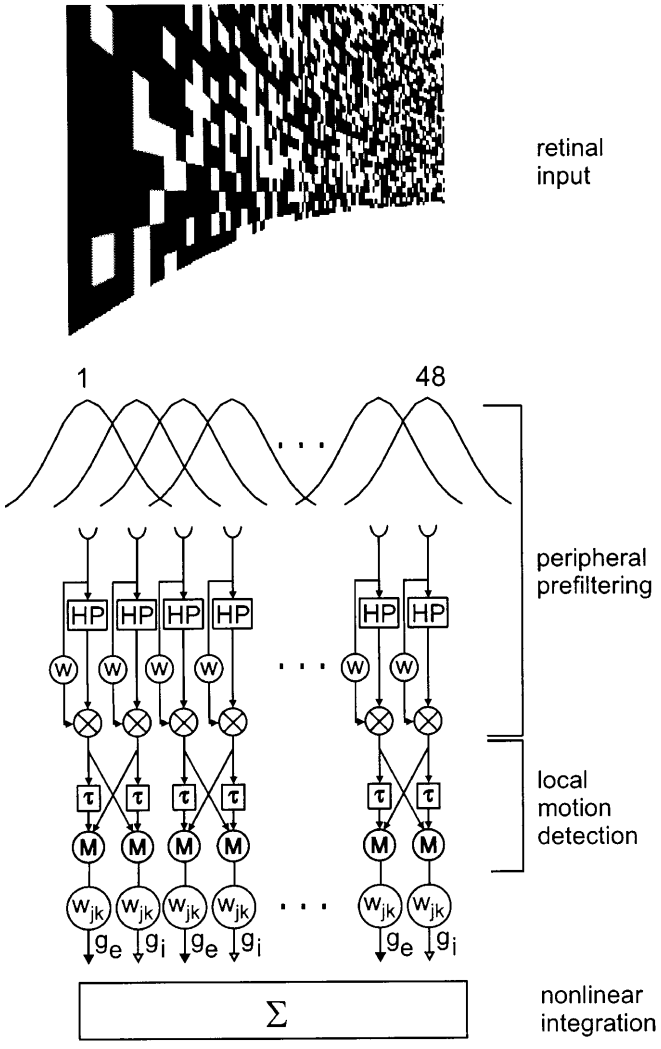

Fig. 2 Schematic of the model of the fly's motion pathway. For the sake of clarity only the horizontal dimension of the model is sketched. The retinotopically organised elements shown are replicated 48 times in the vertical dimension. There are three major processing stages (peripheral prefiltering, local motion detection, non-linear integration of local motion signals). The parameter settings and computations performed at the different processing stages are explained in Materials and methods. *HP* temporal high-pass filter; w, w_{jk} constant weight factors; τ temporal first-order low-pass filter; M multiplication stage of the elementary movement detector; g_e, g_i gain factors of the excitatory and inhibitory output channels of the elementary movement detectors; Σ non-linear integration of the local motion signals

rotations about the vertical axis of the animal (Hausen 1981). This hypothesis is based on the mirror-symmetrical input organisation of those flight steering muscles which are assumed to mediate turns of the animal around its vertical axis (Heide 1983; Egelhaaf 1989).

Based on their response properties, the HS cells can be considered a good starting point for an electrophysiological analysis of the neural representation of behaviourally generated optic flow. Here we focus on the HSE cell and ask how it represents optic flow experienced by monocular animals on a series of walking paths, especially on the average walking path as obtained in behavioural experiments (Kern and Egelhaaf 2000). We have suggested that this average trajectory results from a state of optomotor equilibrium in monocular animals.

The electrophysiological results will be compared to the output of a model of the fly's optomotor system. The elements of this model (Fig. 2) already have been used to reproduce a host of electrophysiological data in previous studies (review: Egelhaaf and Borst 1993a). Although the model can explain a broad range of neuronal response properties, it has not yet been tested with optic flow experienced by the animal during unrestrained locomotion. We show here that the response of the HSE cell and of the model fluctuate around the resting potential, if the retinal image motion corresponds to the optic flow evoked on the average walking path of monocular flies. This finding corresponds well with the proposed state of monocular optomotor equilibrium in monocular flies walking along the mean trajectory.

Materials and methods

Dissection of the animals and electrophysiological recording

Female flies of the genus *Lucilia* were used in all experiments. The animals were bred in our laboratory culture. To avoid in-breeding, the culture was refreshed several times a year with animals caught in the wild. The dissection of the 1- to 2-day-old animals for electrophysiological experiments followed the routines conventionally used in our laboratory (e.g. Warzecha et al. 1993). Alignment of the flies' eyes with the stimulus device was achieved according to the symmetry of the deep pseudopupil (Franceschini and Kirschfeld 1971). Intracellular recordings from the HSE cell in the right optic lobe were made using electrodes which were pulled from borosilicate glass (GC100TF10, Clark Electromedical) on a Brown-Flaming Puller (P-97, Sutter Instruments). When filled with 1 mol l^{-1} KCl they had resistances of 30–60 MΩ. Recordings were made with standard electrophysiological equipment (room temperature between 21 °C and 26 °C). Signals were sampled at a rate of 2 kHz (I/O card DT 2801A, Data Translation) using programs written in ASYST (Keithley Instruments). Data were stored at the sampling frequency and also in a down-sampled version (200 Hz) using time averages of 5 ms. The HSE cell was identified on the basis of physiological criteria, i.e. by its response mode, its preferred direction of motion in the contralateral and ipsilateral visual field, and the location of the receptive field.

Generation of visual stimuli

General procedures

Visual stimuli were generated on an SGI-O2 workstation with the customised application *Vfly* as an extension of the commercial virtual reality software *RealAxScene/Realtime* (a realtime virtual reality modelling/simulation system based on SGI-Performer, REALAX Sofware).

In order to obtain optic flow as experienced by a monocular fly with the right eye open walking in our behavioural setup, a simulated camera was moved in a virtual cylindrical arena of the same size (height 0.29 m, diameter 0.5 m) and with the same random texture (square elements with a side length of 2 mm) as the real arena (Fig. 1A; Kern and Egelhaaf 2000). The camera's field of view always was from 0° to 60° in azimuth. In elevation, the field of view either was from −60° to +60° (visual stimuli corresponding to Figs. 4, 5A, 7) or from −30° to +30° (visual

stimuli corresponding to Figs. 5B, 6). 0°/0° corresponded to the fly's frontal midline at the equator of the eye. The visual stimulus thus covered the most sensitive part of the receptive field of the right HSE cell. The camera was moved along a given trajectory at the height of the walking flies' eyes, i.e. 4 mm above the floor. The position and the azimuth of the camera were updated at a frequency of 100 Hz. Pictures of the visual surround were taken at the same frequency. The *Vfly* application uses an angle-preserving perspective projection to map the simulated 3D environment.

Calculation of the trajectories

The virtual camera was moved on ten different trajectories (T1–T10). T1–T3 and T5–T7 were derived from behavioural data. T4 corresponds to a straight walk directly towards the wall and is used as a reference trajectory. T8–T10 were obtained from closed-loop model simulations of the fly optomotor system and will be introduced later (see section Model simulations). In the preceding behavioural study (Kern and Egelhaaf 2000) the translational (Fig. 3A) and the horizontal angular (Fig. 3B) velocity as well as the angle γ (Fig. 3C) have been determined with respect to the walking flies' distance from the arena centre. γ is the angle between a line aligned with the longitudinal body axis and the tangent onto the arena wall at the intersection point of this line with the arena wall (see inset of Fig. 3C); γ, in other words, defines how the animal is oriented with respect to the wall. With the exception of the arena centre, γ therefore controls at a given position of the fly within the arena, whether the fly is looking at close or distant parts of the arena wall. Because optic flow due to translation depends on the distance between the eye and the structures in the environment (Gibson 1950), it depends on the angle γ. The impact of γ on the optic flow component induced by translation of the animal is strongest near the arena wall. We therefore calculated trajectories T1–T7 *backwards* from a common position 3 mm from the arena wall with γ set to values covering most of the range determined in the behavioural study (Fig. 3C).

Trajectories T1–T3

For the trajectories T1–T3 γ at the *final* position of the trajectories was calculated employing 3rd-order polynomials fitted to the behavioural data, i.e. to the median (T1, $\gamma = 135.7°$) as well as to the 1st (T2, $\gamma = 118.5°$) and 3rd (T3, $\gamma = 146.5°$) quartiles of γ. Third-order polynomials were also fitted to the distance dependent translational and angular velocity of the walking flies (Fig. 3A, B). Employing these polynomials, the position and azimuth of the fly along T1-T3 were calculated at time intervals of 10 ms. The trajectories were calculated backwards, i.e. starting at their *final position* close the arena wall. Backward calculation of trajectory data was stopped either when the new position was closer than 30 mm to the arena centre (T3), or when the trajectory crossed a line through the arena centre that is perpendicular to the connecting line between the arena centre and the trajectory's *final* position (i.e. the starting point of the reconstruction; T1, T2). The *starting* position of the trajectory (i.e. the final point of the reconstruction) was thus different for T1–T3 and the trajectories had different lengths (pictograms in Fig. 4).

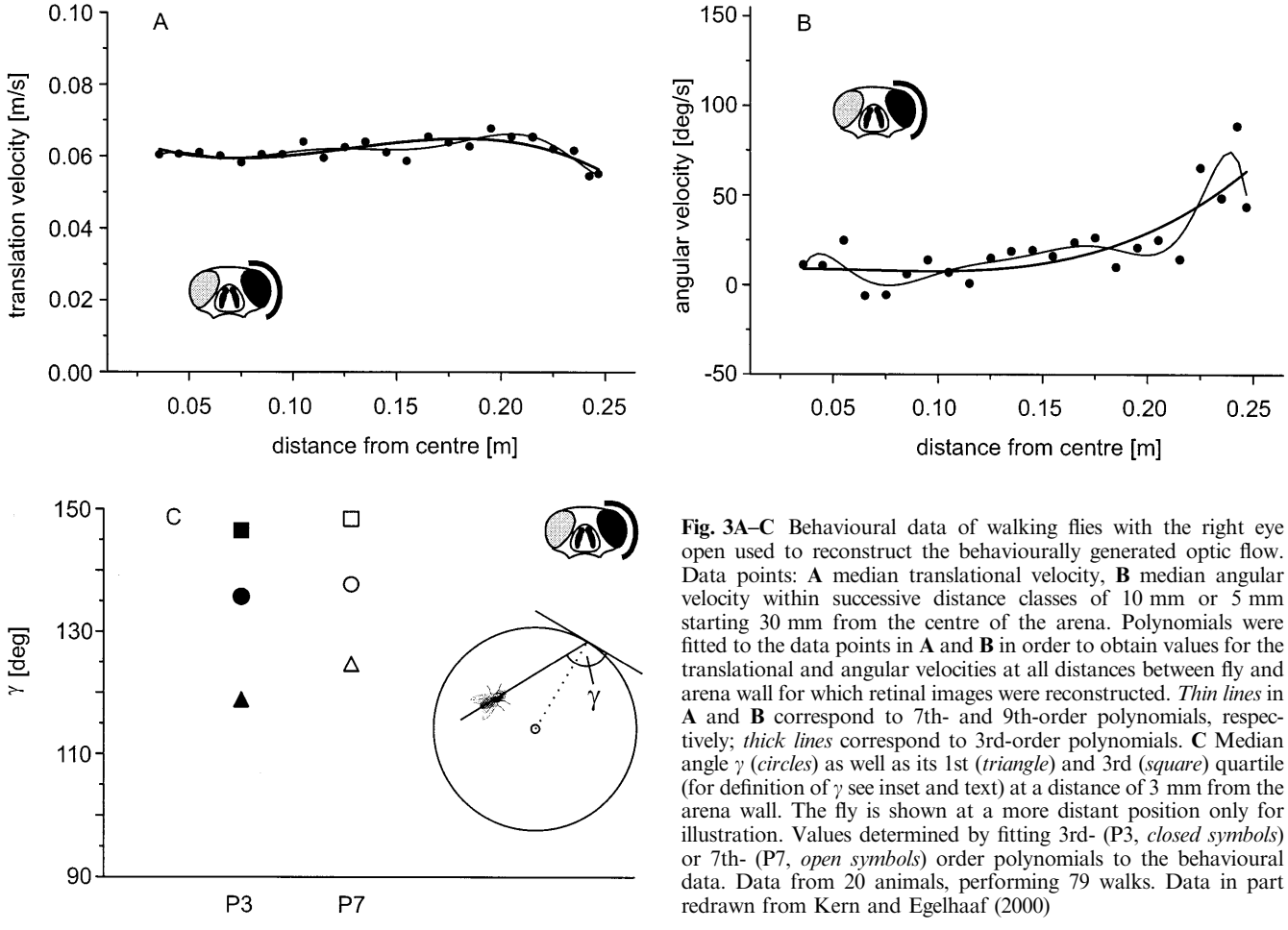

Fig. 3A–C Behavioural data of walking flies with the right eye open used to reconstruct the behaviourally generated optic flow. Data points: **A** median translational velocity, **B** median angular velocity within successive distance classes of 10 mm or 5 mm starting 30 mm from the centre of the arena. Polynomials were fitted to the data points in **A** and **B** in order to obtain values for the translational and angular velocities at all distances between fly and arena wall for which retinal images were reconstructed. *Thin lines* in **A** and **B** correspond to 7th- and 9th-order polynomials, respectively; *thick lines* correspond to 3rd-order polynomials. **C** Median angle γ (*circles*) as well as its 1st (*triangle*) and 3rd (*square*) quartile (for definition of γ see inset and text) at a distance of 3 mm from the arena wall. The fly is shown at a more distant position only for illustration. Values determined by fitting 3rd- (P3, *closed symbols*) or 7th- (P7, *open symbols*) order polynomials to the behavioural data. Data from 20 animals, performing 79 walks. Data in part redrawn from Kern and Egelhaaf (2000)

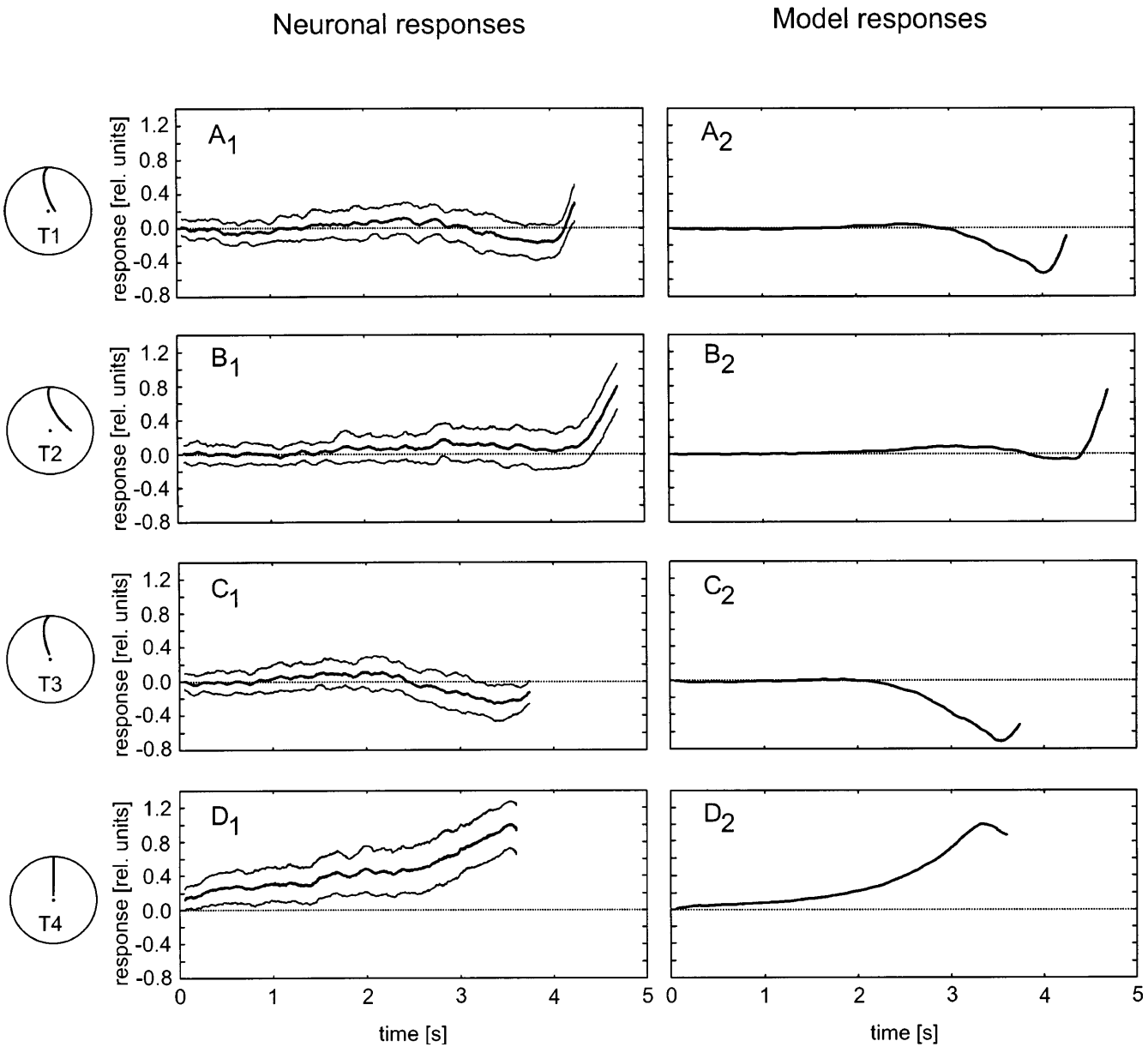

Fig. 4 Time-courses of the average responses of eight HSE cells (*left*, $\mathbf{A_1}$–$\mathbf{D_1}$) as well as of the HSE cell's model counterpart (*right*, $\mathbf{A_2}$–$\mathbf{D_2}$) to the optic flow elicited on the eyes on different walking tracks (T1–T4, see pictograms). T1–T3 were reconstructed using 3rd-order polynomials to fit the behaviourally determined translational and rotational velocities (see Fig. 3). They correspond to the following settings of γ at the distance of 3 mm to the arena wall: 135.7° (median, *T1*), 118.5° (1st quartile, *T2*), 146.5° (3rd quartile, *T3*). T4 is used as a reference stimulus and corresponds to straight walk at a translational velocity of 0.06 m s^{-1}. The responses of the HSE cell and the model cell are given with respect to their activity before motion started (reference level). Responses were normalised to the maximum response to T4 of the HSE cell or the model neuron, respectively, after low-pass filtering the responses using a 100 ms running average. In $\mathbf{A_1}$–$\mathbf{D_1}$ *thick lines* denote average responses, *thin lines* denote standard deviation. The HSE cells' reference levels correspond to membrane potentials in a range from −38.2 mV to −44.7 mV

Trajectory T4

γ at the *final* trajectory position was set to 90° when calculating T4. The translational velocity was fixed at 0.06 m s^{-1}, corresponding approximately to the mean walking velocity of the flies (Fig. 3A), while the angular velocity was set to 0° s^{-1}. These parameter settings correspond to an animal that walks straight from the arena centre towards the arena wall.

Trajectories T5–T7

These trajectories (see pictograms in Fig. 5B) were calculated in the same way as T1–T3. However, higher-order polynomials were fitted to the behavioural data (for details see legend of Fig. 3). γ at the *final* positions of the trajectories amounted to 137.7° (T5; median), 124.3° (T6; 1st quartile), and 148.4° (T7; 3rd quartile).

Presentation of visual stimuli

The reconstructed retinal images were presented on a 15″ computer monitor (Nokia 449Xa Plus Multigraph) which was placed within the receptive field of the HSE cell in the right optic lobe. The frontal and lateral boundaries of the stimulus pattern were at an angular position of 0° and 60° with 0° corresponding to the frontal

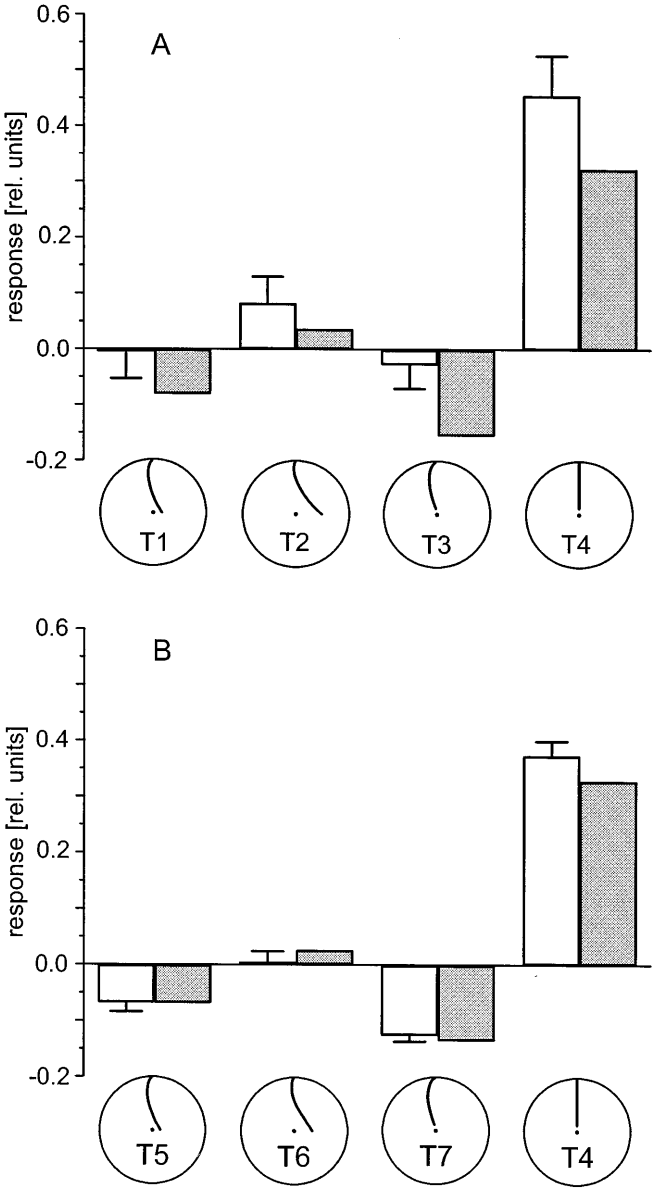

Fig. 5A, B Time-averaged responses of HSE cells (*white columns*) and the HSE cell's model counterpart (*grey columns*) to the optic flow elicited on the eyes on seven different walking trajectories (see pictograms). For description of T1–T4 see legend of Fig. 4. T5–T7 were reconstructed from the same behavioural data as T1–T3 but higher-order polynomials were fitted to the data points (see legend of Fig. 3). They correspond to the following settings of γ at the distance of 3 mm to the arena wall: 137.7° (median, *T5*), 124.3° (1st quartile, *T6*), 148.4° (3rd quartile, *T7*). The same normalisation procedure was applied as in Fig. 4. Time-averages in **A** correspond to the responses shown in Fig. 4. The *bars* denote standard errors. In **A** eight cells, in **B** nine cells were recorded from. The HSE cells' reference levels correspond to membrane potentials in a range from **A** −38.2 mV to −44.7 mV, **B** −37.6 mV to −55.8 mV

midline of the animal. The dorsal and ventral boundaries of the stimulus pattern were at an elevation of 60° and −60° (visual stimuli corresponding to Figs. 4, 5A, 7) or 30° and −30° (visual stimuli corresponding to Figs. 5B, 6) relative to the horizon. The respective pattern sizes were 80 × 160 pixels and 160 × 160 pixels, resulting in average spatial resolutions of 0.75°/pixel and 0.375°/pixel. Visual stimuli were presented at a frame rate of 100 Hz. Pattern contrast was 98% with a mean luminance of 27 cd m^{-2}. Prior to presentation of the images obtained from a given trajectory a stationary image was shown for 1 second. This image corresponded to either the first frame obtained from the respective trajectory (visual stimuli corresponding to Figs. 4, 5A, 7), or was a grey square (10 cd m^{-2}; visual stimuli corresponding to Figs. 5B, 6). There was an interval of at least 10 s between the presentations of different image sequences. Not all image sequences obtained from T1–T10 were replayed to each cell. Rather, the retinal image sequences obtained from T1–T4 and T8–T10, were presented repeatedly in pseudo random order to one set of HSE cells, whereas the image sequences obtained from T4–T7 were presented in pseudo random order to a different set of HSE cells.

Data analysis

For each image sequence presentation the mean membrane potential of the HSE cell was determined in a 250-ms epoch starting 750 ms after recording onset. Response amplitudes evoked by optic flow are given with respect to this reference level. The mean time-dependent responses of all cells to a given image sequence were averaged and temporally low-pass filtered by a running average (width 100 ms) before plotting. Neuronal responses compared to model data (Figs. 4, 5, 7) were normalised to the maximal amplitude of the response to the optic flow elicited on the straight trajectory (T4). Data evaluation was done with Matlab (The Mathworks).

Model simulations

Our model is an elaboration of models previously established to explain various aspects of motion detection by the fly visual system (see Introduction). It is a hybrid of algorithmic components and components which represent a simple equivalent circuit of a nerve cell. The peripheral part of the motion detection pathway, i.e. the peripheral filters corresponding to the retina and the first visual neuropil, as well as the motion detection process itself were modelled by linear filters, the outputs of which interact with each other by simple mathematical operations. Hence, although the output of this part of the model was meant to fit the output of the local motion detectors of the fly, it was not intended to approximate the cellular operations which are responsible for the neuronal response properties in any detail. Spatial pooling of the many local motion detectors was achieved by means of a simple equivalent circuit of a patch of membrane, where the positive and negative outputs of the local motion detectors controlled excitatory and inhibitory conductances, respectively. The model output thus can be interpreted as representing the graded postsynaptic potential of the HSE cell.

The model consists of three processing stages which will be referred to as (1) peripheral filtering, (2) local motion detection, and (3) spatial pooling of local motion information (Fig. 2). The input frame size was 240 × 240 pixels, corresponding to a visual field of 60° × 60°. Peripheral filtering started with spatial downsampling of each input frame to an equidistant retinal receptor matrix consisting of 48 × 48 elements; thus, the receptor distance was 1.25°. The input to each receptor was spatially filtered according to the experimentally established spatial sensitivity distribution of the individual photoreceptors (Smakman et al. 1984) by a two-dimensional Gaussian ($\sigma = 0.75°$). To mimic the phasic response properties of output cells of the fly's first visual neuropil (Laughlin 1994; Juusola et al. 1996), the photoreceptor output was temporally filtered with a first-order high-pass filter (time constant: 50 ms) and added to the unfiltered photoreceptor output after the latter was weighed by 0.15. The resulting signals were fed into correlation-type motion detectors, which have been shown to explain many aspects of the local motion detector (EMD) responses in the fly's visual system (review: Egelhaaf and Borst 1993a). Each detector consisted of two mirror-symmetrical subunits (Fig. 2). The subunits received their inputs from two input channels being neighbours along the horizontal axis of the model

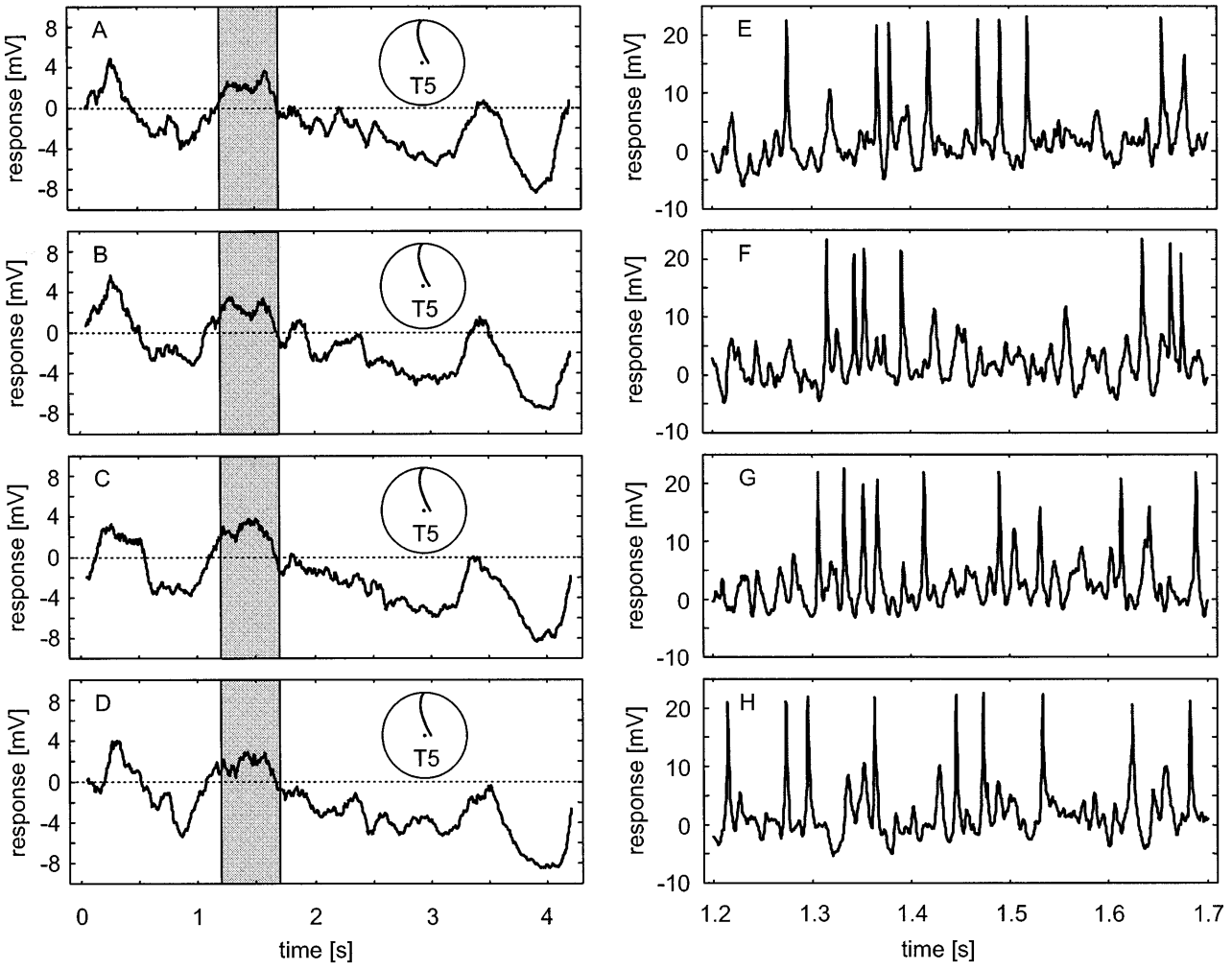

Fig. 6A–H Individual responses on a coarse (*left*) and a fine (*right*) timescale. **A–D** Responses of the HSE cell to repetitive stimulation with optic flow induced on the eyes when a fly walks on T5 (see insets). Responses (time averages of 5 ms from data sampled at 2 kHz) were low-pass filtered using a 100 ms running average. **E–H** Sections of the responses plotted in (**A–D**, *shaded areas*) with a temporal resolution of 0.5 ms and without filtering. Note different time scales of plots. Reference levels correspond to membrane potentials in a range from −37.9 mV to −38.8 mV

retina. In each subunit the signal was temporally filtered with a first-order low-pass filter (time constant: 100 ms) and multiplied with the unfiltered signal of the neighbouring input. The two subunit outputs were excitatory and inhibitory with respect to the model HSE cell which spatially pooled these outputs. The excitatory and inhibitory subunit outputs were assumed to modulate the membrane conductances (g_e, g_i) in the model HSE cell with reversal potentials $E_e > 0$ and $E_i < 0$, respectively. 0 corresponded to the resting potential of the cell. The membrane conductances introduced a non-linearity into the model HSE cell which was partly responsible for the above-mentioned gain control (Borst et al. 1995). To adjust the spatially distributed motion detector input of the model HSE cell to the spatial sensitivity distribution of the HSE cell (Hausen 1982b), the subunit outputs were weighed according to their position within the two-dimensional detector array. We used a two-dimensional phase-shifted spatial $\sin^2$ function for the approximation of the sensitivity distribution. With w_{jk} representing the local sensitivities of the HSE cell at the spatial coordinates j and k, its output was calculated in the following way:

$$R = \left(\sum_{1}^{j}\sum_{1}^{k} w_{jk}(E_e \times g_e - E_i \times g_i)\right) \Big/ \left(\sum_{1}^{j}\sum_{1}^{k}(w_{jk}(g_e + g_i + g_0))\right), \quad (1)$$

Since membrane conductances cannot become negative, g_e and g_i were set to zero, if the output of the corresponding detector subunits was less than zero. Based on previous combined electrophysiological and model studies on fly motion detection (Egelhaaf et al. 1989) it was assumed that $|E_i| = 0.94 \times |E_e| \cdot g_0$ can be interpreted as the leak conductance of the model HSE cell when it is not stimulated. Equation 1 controls the output gain of the model cell in accordance with electrophysiological findings in HS cells (Borst et al. 1995). The parameters were adjusted according to earlier studies where simple stimuli were systematically varied to characterise the peripheral filtering of the retinal input, the process of motion detection and the non-linear integration of local motion information (Egelhaaf et al. 1989; Borst et al. 1995). The model parameters were not optimised to fit as closely as possible the neuronal responses to optic flow as was used for visual stimulation in the present study. As for the electrophysiological data, the reference level of the model responses was determined as the mean response during a 250-ms time interval starting 750 ms after presentation of the first stationary image. The model responses also were normalised to the maximal amplitude of the response to the optic flow elicited on the straight trajectory (T4).

Closed-loop simulations – generation of T8–T10

The responses of the HSE cell to the image sequences corresponding to T1–T3 and T5–T7 will be used to decide whether the

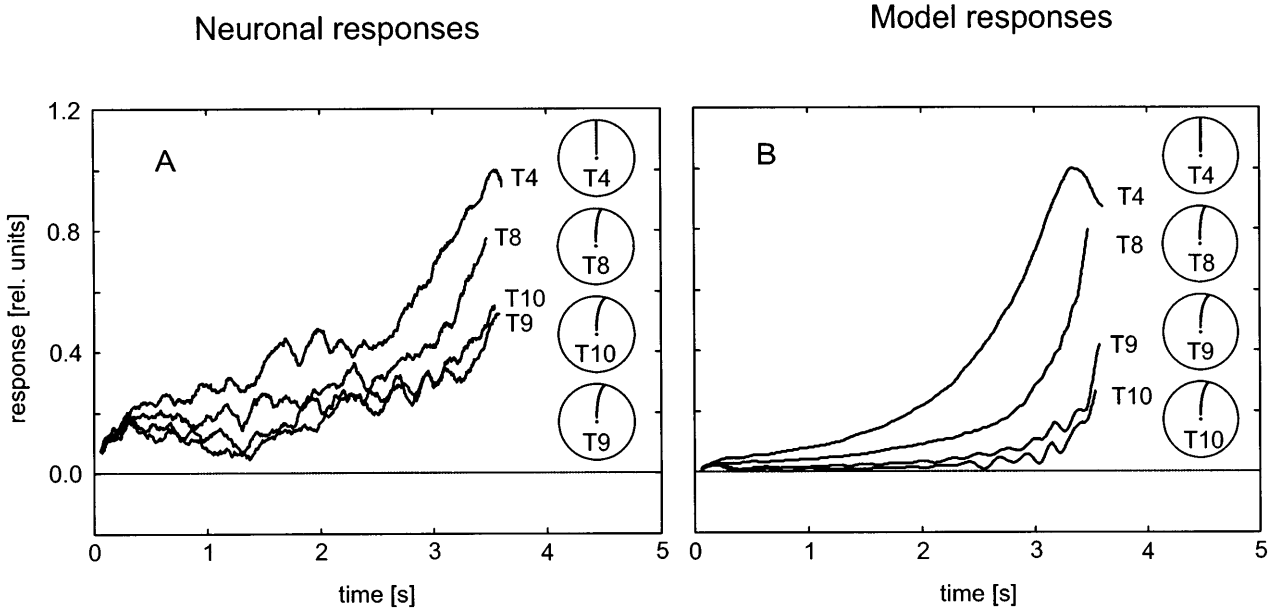

Fig. 7 Time-courses of the average responses of five HSE cells (**A**) as well as of the HSE cell's model counterpart (**B**) to the optic flow elicited on walking trajectories as obtained from closed-loop model simulations (T8–T10, see insets) or, as a control, on a straight path (*T4*; see inset). In the closed-loop simulations the output of the model was used to control the rotational velocity of a virtual fly. The (open loop) translational velocity depended on the distance to the arena wall in accordance with the behavioural data (Fig. 3). Any difference between the model cell's response and the response level immediately before the virtual fly started walking led to rotations aimed at zeroing this difference. Parameters of the feedback loop were varied. T8: gain 5, no low-pass filter; T9: gain 25, first-order low-pass filter with 250 ms time-constant; T10: gain 50, first-order low-pass filter with 500 ms time-constant. The same normalisation procedure was applied as in Fig. 4. The HSE cells' reference levels correspond to membrane potentials in a range from −38.7 mV to −46.1 mV

average walking trajectory of monocular flies complies with the idea of a monocular optomotor equilibrium. We do not know, however, whether the flies – on average – aspired an optomotor equilibrium in the behavioural experiments (see Discussion). As a reference we therefore performed closed-loop simulations. In these simulations a 'virtual fly' aimed at an optomotor equilibrium, i.e. any deviation of the actual model response from the reference level led to rotations of the virtual fly around its vertical body axis in the next time step of the simulation. The direction of rotation was as to reduce the model response.

The virtual fly started walking at a position 30 mm from the arena centre (see pictograms in Fig. 7). The angle γ at the starting position was set to 90°. The translational velocity of the virtual fly at each time step was calculated according to the 3rd-order polynomial fitted to the behavioural data (Fig. 3A). It did not depend on the model output (open-loop conditions). In contrast, the virtual fly's angular velocity at a given time depended on the output signal of the model at the preceding time step (closed-loop conditions). The simulation was stopped when the virtual fly came as close as 3 mm to the arena wall.

The closed-loop model simulations were performed under three different coupling conditions between the model output and the angular velocity of the virtual fly and, thus, the rotational component of optic flow in the next time step. Either the output signal of the model HSE cell was just weighed with a constant coupling coefficient before it was fed back to the angular velocity, i.e. the retinal input. Alternatively, it was first temporally low-pass filtered (for details see legend of Fig. 7). Low-pass filtering of the HSE cell output was motivated by the finding that the frequency response of the yaw torque of the fly has its cutoff at much lower frequencies than that of the HSE cell (Egelhaaf 1987) and was successfully employed in an analysis of the stability properties of optomotor course control of the fly (Warzecha and Egelhaaf 1996). In all cases the feedback gain was set to the largest value that did not generate instabilities. The time series of positions and orientations of the longitudinal body axis of the virtual fly during the corresponding simulations were stored and used as trajectories T8–T10 which were the basis for the electrophysiological replay experiments shown in Fig. 7.

Results

In a previous paper (Kern and Egelhaaf 2000) it was shown that, on average, the walking trajectories of monocularly blinded animals are slightly curved. The average trajectory was characterised by the translational and rotational velocities of the animal and its orientation with respect to the wall of the circular arena (γ, for definition see Fig. 3C and Materials and methods). In the present account, the retinal input of the fly as perceived while walking on the average trajectory was reconstructed and replayed to flies in electrophysiological experiments. In order to consider the scatter of the behavioural data due to the variability of the flies' behaviour, we did not only reconstruct the image sequence corresponding to the median values characterising the average trajectory. Rather we also reconstructed image sequences corresponding to the 1st and 3rd quartiles of γ at the final position of the average trajectory. In addition, we approximated the values of the trajectory (T) characterising parameters in two ways by fitting either low (T1–T3) or high (T5–T7) order polynomials to the data points. As a reference stimulus, the images corresponding to a straight walk (T4) were reconstructed and presented to the HSE cell in the fly optomotor system. The reconstructed retinal images

were also fed into a model of the fly's optomotor system and the responses of real cell and model equivalent were compared to each other. In addition to visual stimuli derived from behavioural data we also used stimuli derived from closed-loop model simulations of a virtual fly aspiring a monocular optomotor equilibrium. The activity of 17 HSE cells was recorded sufficiently long to be included in the analysis.

Responses to trajectories derived from behavioural data

When the fly approached the wall on the reference trajectory (T4), i.e. on a straight course, the HSE cell continually depolarised and reached its maximum depolarisation close to the wall (Fig. $4D_1$). On average, the response amplitude was positive with respect to the reference membrane potential determined before the motion onset (Fig. 5). In contrast, the optic flow experienced on the trajectories T1-T3 led to comparatively small responses. The time-dependent membrane potential did not deviate much from the reference level (Fig. 5A). The responses tended to fluctuate around the reference level and only towards the end of the trajectory, i.e. when the fly was close to the wall, the membrane potential was more depolarised (Fig. $4A_1$, B_1) or hyperpolarized (Fig. $4C_1$). Thus, clockwise rotation of the fly around its vertical axis while walking towards the arena wall led most of the time to a reduction of the HSE cell response as compared to the response to retinal image motion on the straight trajectory. The degree of reduction depends on the angle γ, the parameter that slightly differs for T1, T2, and T3.

Similar results were obtained when the image sequences obtained from trajectories T5–T7 were presented to the HSE cell. The membrane potential also fluctuated around the resting level, though response modulations were somewhat larger (for T5 see Fig. 6A–D; time-courses for T6, T7 not shown). The stronger modulations as compared to those of responses while presenting image sequences obtained from T1–T3 can be explained partly by the differences in modulation depth of the polynomials fitted to the angular velocity data for calculating T1–T3 or T5–T7, respectively (Fig. 3B).

The time-averaged responses to the image sequences obtained from T1–T3 and T5–T7, i.e. from walking trajectories related to the average trajectory as determined in the behavioural study, are considerably smaller than the responses to the optic flow experienced on a straight path (T4; Fig. 5). This holds independently of whether low- or high-order polynomials were used to fit the behavioural data.

The response of the HSE cell might not only depend on the type of trajectory but also on the particular pattern of the arena wall texture seen by the fly. Therefore, as a control, we reconstructed and replayed the retinal images also for the fly walking along T1 but with the arena rotated around its vertical axis by 7.5°. No obvious differences were found in the responses of the HSE cell with the arena pattern at the original or at the modified angular position (not shown).

The optic flow resulting from walking trajectories T1–T7 was also fed into the model of the fly optomotor system. Comparing the model simulations with the corresponding electrophysiological recordings reveals that both were similar with respect to their main qualitative features. The model cell also increasingly depolarised in response to optic flow when the fly walked on a straight path towards the wall (Fig. $4D_2$). The responses of the model cell to the optic flow experienced on T1–T3 also stayed close to the reference level at the beginning of the trajectories and fluctuated around the reference level (Fig. $4A_2$–C_2) in a similar way to the responses of the HSE cell (Fig. $4A_1$–C_1). In addition, the model cell depolarised (Fig. $4B_2$) or hyperpolarized (Fig. $4C_2$) when the fly came close to the wall, comparable to observations on the HSE cell. Also, the time-courses of the responses of the HSE cell and the model to image sequences obtained from T5–T7 were alike (not shown). Moreover, as with the HSE cell, the model's average responses to the optic flow experienced on T5–T7 were very similar to the responses to the optic flow experienced on T1–T3 (Fig. 5). The similarity of cellular and model responses to behaviourally generated optic flow corroborates earlier conclusions based on much simpler motion stimuli, that the model of the fly's optomotor system can explain many features of the neuronal responses quite well. The similarity between real cell data and model data does not depend critically on the exact model parameter settings.

From the results presented so far it can be concluded that on the average trajectory of monocularly blinded animals a state of optomotor equilibrium is approximately reached, at least along most of the trajectory. The conclusion is based on the finding that the response of the HSE cell as an output element of the fly's optomotor system and the response of its model equivalent fluctuate around the reference level under the respective stimulus conditions.

This conclusion basically pertains to the responses of the HSE cell on a relatively coarse timescale of some hundreds of milliseconds, i.e. on down-sampled and temporally low-pass filtered data. If scrutinised on this timescale the averaged responses to a given stimulus from different cells (not shown) and even individual responses to repeated presentations of this stimulus look very similar (Fig. 6A–D). In contrast, the responses look very different on a much finer timescale (i.e. unfiltered data sampled at 2 kHz) and it is hardly possible to infer from the individual responses that they were all induced by the same motion trace (Fig. 6E–H). This variability does not occur in our current model of the fly motion pathway, since, in contrast to real neurons, the constituent elements of the model do not contain any stochastic sources.

Responses to trajectories derived from closed loop simulations

The trajectories calculated from the data derived from monocular walking flies led to responses of the HSE cell and its model equivalent that are in accordance with the idea of a monocular optomotor equilibrium. However, towards the end of the trajectories, i.e. when the fly was close to the wall, both the real and the model cell's membrane potential might deviate considerably from the reference potential. The difference can be positive when the fly walked on T2, or negative when it walked on T3. This fact indicates that the fly in the two cases either might turn too slowly or too fast in order to cancel out the influence of the optic flow due to forward translation. This behavioural performance of the fly might result either from its inability to control its turning velocity sufficiently well, or simply from the fact that the fly does not aspire an optomotor equilibrium. We performed closed-loop model simulations in order to find out how well a system aimed at an optomotor equilibrium is able to achieve it.

The optic flow experienced by the walking flies depended on both their translational and rotational velocity. Therefore, an optomotor equilibrium might be achieved by changing either of the two walking parameters. The translational velocity of monocular flies had been found to be rather independent of the animals' distance to the arena wall (Fig. 3A), whilst the angular velocity changed dramatically (Fig. 3B). Therefore, as a first approximation to a real behavioural closed-loop situation, the output of the model HSE cell was fed back only to the angular velocity of a virtual fly walking towards the arena wall, whereas the translational velocity was unaffected by the response of the model cell. In this way we avoided to make assumptions about the way in which the translational velocity may depend on retinal stimulation. The feedback loop was designed so as to reduce the response amplitude of the model HSE cell. The simulations were performed with different parameter settings for the feedback loop (see legend of Fig. 7), resulting in three different trajectories (T8–T10). While the virtual fly was distant to the wall, the response of the model cell deviated only little from its reference level (Fig. 7B). However, even under closed-loop conditions the model cell depolarised in the final course of all trajectories. This depolarisation was independent of the parameter settings, while its amplitude was smallest when the output of the model HSE was temporally low-pass filtered and the feedback gain relatively large. We did not find parameter settings for the virtual fly, where this depolarisation did not occur under closed-loop conditions. Note that the feedback gain was always set to the largest value possible without generating instabilities. In any case, the depolarisation was smaller than the one induced during a straight approach of a fly towards the wall (T4). Similar responses were obtained from the HSE cell when stimulated with the image sequences corresponding to T8–T10 (Fig. 7A).

In conclusion, depolarizations of the HSE cell occur even under closed-loop conditions, when the model is designed to approach a state of optomotor equilibrium as closely as possible. These findings reveal, that even the depolarizations observed in the replay experiments with optic flow evoked on T1–3 and T5–7 are in accordance with the interpretation that these walking trajectories reflect a state of optomotor equilibrium of the fly.

Discussion

In the present study the hypothesis is tested that flies with one eye occluded walk, on average, on a trajectory which corresponds to a state of optomotor equilibrium. This equilibrium implicates for monocular flies that the optomotor system does not signal a deviation from a straight course, although the fly walks on a slightly curved trajectory. This hypothesis was put forward in a previous behavioural analysis on flies where only one of the eyes could perceive the visual consequences of the fly's locomotor activity (Kern and Egelhaaf 2000). The hypothesis was tested, on the one hand, by recording from a neuron, the HSE cell, which has been proposed previously to play a decisive role in optomotor course control (see Introduction) and, on the other hand, by computer simulations of a network model of the fly's optomotor system. On average, the outputs of the HSE cell and its model equivalent are close to the reference level determined before motion onset when confronted with optic flow as experienced on the average trajectory of monocular flies. The responses are thus much smaller than during straight walk. We therefore conclude that the average walking trajectory of monocular flies corresponds to an optomotor equilibrium. This conclusion can be drawn independent of the exact procedure applied to fit the behavioural data in order to calculate the trajectories for retinal image reconstruction. The conclusion is further corroborated by the results of closed-loop model simulations. Even under conditions where the model is tuned to minimise the difference between response and reference level the two signals might deviate from each other. The magnitude of deviation is in the range of what has been found for stimuli derived from behavioural data.

Variability of neuronal responses

It is obvious from the neuronal responses analysed in the present study that on a fine timescale neuronal variability is very large and renders it virtually impossible to infer the time-course of the motion stimulus from the neuronal response. On the other hand, on a coarse timescale, there is much less variability and even individual responses elicited by the same image sequences look very similar. Neuronal variability in the HSE cell under the present behaviourally relevant stimulus conditions does not differ from that found

under more artificial conditions (A.-K. Warzecha, unpublished observations). It should be emphasised in this context, that the optic flow derived from the average walking traces changes only relatively slowly in time. Hence, to encode such slow changes there is no need for a high temporal precision of neuronal activity on a millisecond timescale. Since the average traces of locomotion are artificial in the sense, that they represent only the average of real traces of locomotion, this result cannot be taken as evidence that no faster motion transients occur in the optic flow induced by realistic movements of the animal. This qualification especially holds if flying flies are considered that are able to perform steering manoeuvres within less than 20 ms (Hateren and Schilstra 1999; Schilstra and Hateren 1999). We are therefore currently analysing neuronal responses to optic flow elicited on the eyes in various behavioural contexts and a range of three-dimensional environments.

Approaches to neuronal processing of behaviourally relevant information

Neuronal processing of sensory information is usually analysed by using stimuli that are simpler, with respect to both their dynamical and spatial complexity, than the stimuli an animal encounters in natural situations. Although relatively simple stimuli might be essential for systems analysis to unravel the mechanisms underlying neuronal computation, they do not easily allow us to make predictions how these mechanisms perform under natural behavioural conditions. In principle, it would be advantageous to monitor neuronal activity during normal behaviour. However, monitoring neuronal activity in behaving animals is only possible in some animals under very specific conditions, for instance while the animals are kept relatively immobile or while moving only slowly (e.g. Wolf and Pearson 1987; Newsome et al. 1989; Hammer 1993; Büschges et al. 1994; Staudacher and Schildberger 1998). So far, it is not possible to record single-cell activity intracellularly in most freely moving animals (see, however, Wilson and McNaughton 1993). To get an idea of how sensory information is processed during behaviour, the second best approach is to confront the animal in electrophysiological experiments with stimuli which are identical to that evoked in previous behavioural situations. For visual motion processing, the respective retinal images sequences can be obtained in two ways: (1) by having a camera mounted on a freely moving animal, or (2) by measuring the trajectories of behaving animals in a known environment and by reconstructing the visual surround from the animal's point of view. While the first approach is only possible in relatively large animals which can carry a camera, and is thus not feasible when working on flies, the latter one can be employed with smaller animals as long as the behaviour to be observed is spatially confined within the range of the measuring system. While both approaches to reconstruct the visual input of a moving animal have already been employed (Passaglia et al. 1997; Zeil and Zanker 1997), so far they were used only to feed models of the analysed visual systems with natural visual input. In this respect, the present study differs from the above-mentioned ones. The optic flow generated in a three-dimensional environment was not only used as input to a model of the fly's optomotor system, but also to stimulate a neuron of the fly's optomotor system in electrophysiological experiments. A similar approach to address the problem of how behaviourally generated visual motion is encoded by the fly nervous system was already employed before (Warzecha and Egelhaaf 1997; Kimmerle 1999). However, in these studies the behaving flies were much more restrained than in the behavioural study the current electrophysiological experiments are based on. In the previous studies the behavioural experiments were done in a flight simulator on stationary flying flies (Warzecha and Egelhaaf 1997; Kimmerle 1999).

There is one cardinal problem inherent to all electrophysiological experiments on restrained animals. The question is to what extent the analysed cells are in a similar state as in the intact, behaving animal on which the corresponding behavioural experiments were done before. Although this question can never satisfactorily be answered, since monitoring single-cell activity inevitably requires an invasive experiment, there are indications that the visual system of the fly – at least up to the level of the third visual neuropil where the HSE cell resides – is not in a principally different state under restrained and behavioural conditions. Responses of a motion sensitive neuron in the third visual neuropil of the fly and, thus, at the same processing level as the HSE cell, are virtually indistinguishable when recorded in immobilised flies (as in our study) and when recorded in tethered flying flies (Heide 1983). Hence, there are currently no reasons to assume that the response of the HSE cell as analysed in the present study do not equal those in the intact behaving animal.

It should be noted that the motion sequences which were used as stimuli in the present study do not correspond to the retinal input that has ever been perceived by a real fly. Rather the motion sequences correspond, according to the question underlying the present study, to mean trajectories derived from many walks and many flies. Moreover, as a reference a motion sequence was used corresponding to a completely straight walk at constant forward speed and thus to a situation which never occurs. Despite these qualifications the present approach seems most valuable to us for two reasons. First, it allows us to characterise neuronal elements with behaviourally relevant optic flow. Second, it offers the possibility to systematically manipulate this optic flow.

Model of the fly optomotor system

The electrophysiological results obtained with the HSE cell were compared to the responses of a model of the

fly's optomotor system. Qualitatively, both responses fit very well for all tested stimulus conditions. This finding is in line with the results of earlier studies on motion information processing in the fly optomotor system where simpler stimuli than in the present study have been employed: The model in its present form is able to reproduce the *average* responses of the HSE cell even under rather complex stimulus conditions. Hence, the model output can be interpreted as the average stimulus-induced postsynaptic potential of the HSE cell. Individual responses that underlie neuronal variability can not be simulated in the model's current form, however. The model neither contains stochastic signal sources as present almost everywhere in the nervous system nor does it possess active processes, such as are responsible for spike generation. In the present account we just wanted to explain the stimulus-induced component of the responses, rather than all the subtleties of their time-course, such as random potential fluctuations or the timing of individual spikes. These features of neuronal responses in the fly visual system are in the focus of parallel projects in our lab as well as in other groups (review: Egelhaaf and Warzecha 1999).

The consideration of stochastic signal sources and active processes in the model would be insufficient to explain individual walking tracks of the fly. In contrast to our model the behaviour of real flies is affected by determinants others than the visual stimulus. As we outlined in the previous paper (Kern and Egelhaaf 2000) flies are not forced to achieve an optomotor equilibrium at any instance of time. They rather can walk straight or on curved paths due to necessities and processes not obvious to the experimenter. Despite these limitations, the model helps to understand motion information processing in the fly brain. Closed-loop simulations as introduced here will support further progress in the future.

Acknowledgements We are indebted to J.P. Lindemann for writing and developing the stimulus presentation program used in the present study. Thanks also to K. Runte for writing earlier versions of this program. We are much obliged to U. Witte for the basic ideas on the hard- and software concept of the stimulus program. Many thanks to A.-K. Warzecha who wrote the program for data acquisition and to C. Petereit who did part of the electrophysiological recordings. Finally, we would like to thank H. Krapp, R. Kurtz, and A.-K. Warzecha for valuable discussions and suggestions on the manuscript. This work was supported by the DFG.

References

Borst A, Egelhaaf M, Haag J (1995) Mechanisms of dendritic integration underlying gain control in fly motion-sensitive interneurons. J Comput Neurosci 2: 5–18

Büschges A, Kittmann R, Schmitz J (1994) Identified nonspiking interneurons in leg reflexes and during walking in the stick insect. J Comp Physiol A 174: 685–700

Egelhaaf M (1987) Dynamic properties of two control systems underlying visually guided turning in house-flies. J Comp Physiol A 161: 777–783

Egelhaaf M (1989) Visual afferences to flight steering muscles controlling optomotor response of the fly. J Comp Physiol A 165: 719–730

Egelhaaf M, Borst A (1993a) A look into the cockpit of the fly: visual orientation, algorithms, and identified neurons. J Neurosci 13: 4563–4574

Egelhaaf M, Borst A (1993b) Movement detection in arthropods. In: Wallman J, Miles FA (eds) Visual motion and its role in the stabilization of gaze. Elsevier, Amsterdam, pp 53–77

Egelhaaf M, Reichardt W (1987) Dynamic response properties of movement detectors: theoretical analysis and electrophysiological investigation in the visual system of the fly. Biol Cybern 56: 69–87

Egelhaaf M, Warzecha A-K (1999) Encoding of motion in real time by the fly visual system. Curr Opin Neurobiol 9: 454–460

Egelhaaf M, Hausen K, Reichardt W, Wehrhahn C (1988) Visual course control in flies relies on neuronal computation of object and background motion. Trends Neurosci 11: 351–358

Egelhaaf M, Borst A, Reichardt W (1989) Computational structure of a biological motion detection system as revealed by local detector analysis in the fly's nervous system. J Opt Soc Am A 6: 1070–1087

Franceschini N, Kirschfeld K (1971) Les phénomnes de pseudopupille dans l'oeil composé de *Drosophila*. Kybernetik 9: 159–182

Geiger G, Nässel DR (1981) Visual orientation behaviour of flies after selective laser beam ablation of interneurones. Nature (Lond) 293: 398–399

Gibson JJ (1950) The perception of the visual world. Houghton Mifflin, Boston, Mass

Götz KG (1975) The optomotor equilibrium of the *Drosophila* navigation system. J Comp Physiol 99: 187–210

Haag J, Borst A (1998) Active membrane properties and signal encoding in graded potential neurons. J Neurosci 18: 7972–7986

Hammer M (1993) An identified neuron mediates the unconditioned stimulus in associative olfactory learning in honeybees. Nature (Lond) 366: 59–63

Hateren JH van, Schilstra C (1999) Blowfly flight and optic flow. II. Head movements during flight. J Exp Biol 202: 1491–1500

Hausen K (1981) Monocular and binocular computation of motion in the lobula plate of the fly. Verh Dtsch Zool Ges 74: 49–70

Hausen K (1982a) Motion sensitive interneurons in the optomotor system of the fly. I. The horizontal cells: structure and signals. Biol Cybern 45: 143–156

Hausen K (1982b) Motion sensitive interneurons in the optomotor system of the fly. II. The horizontal cells: receptive field organization and response characteristics. Biol Cybern 46: 67–79

Hausen K, Wehrhahn C (1983) Microsurgical lesion of horizontal cells changes optomotor yaw responses in the blowfly *Calliphora erythrocephala*. Proc R Soc Lond Ser B 219: 211–216

Hausen K, Wehrhahn C (1990) Neural circuits mediating visual flight in flies. II. Separation of two control systems by microsurgical brain lesions. J Neurosci 10: 351–360

Heide G (1983) Neural mechanisms of flight control in Diptera. In: Nachtigall W (ed) BIONA report. Akademie der Wissenschaften und der Literatur zu Mainz. Fischer, Mainz, pp 35–52

Heisenberg M, Wonneberger R, Wolf R (1978) Optomotor-blind – a *Drosophila* mutant of the lobula plate giant neurons. J Comp Physiol 124: 287–296

Juusola M, French AS, Uusitalo RO, Weckström M (1996) Information processing by graded-potential transmission through tonically active synapses. Trends Neurosci 19: 292–297

Kern R, Egelhaaf M (2000) Optomotor course control in flies with largely asymmetric visual input. J Comp Physiol A 186: 45–55

Kimmerle B (1999) Object detection by the fly *Lucilia*: behavioral experiments in the flight simulator and performance of visual interneurons. Doctoral Dissertation, University Bielefeld

Laughlin SB (1994) Matching coding, circuits, cells, and molecules to signals: general principles of retinal design in the fly's eye. Progress in retinal and eye research, vol. 13, No.1. Pergamon Press. Great Britain, pp 165–196

Newsome WT, Britten KH, Movshon JA (1989) Neuronal correlates of a perceptual decision. Nature (Lond) 341: 52–54

Passaglia C, Dodge F, Herzog E, Jackson S, Barlow R (1997) Deciphering a neural code for vision. Proc Natl Acad Sci USA 94: 12649–12654

Schilstra C, Hateren JH van (1999) Blowfly flight and optic flow. I. Thorax kinematics and flight dynamics. J Exp Biol 202: 1481–1490

Single S, Haag J, Borst A (1997) Dendritic computation of direction selectivity and gain control in visual interneurons. J Neurosci 17: 6023–6030

Smakman JGJ, Hateren JH van, Stavenga DG (1984) Angular sensitivity of blowfly photoreceptors: intracellular measurements and wave-optical predictions. J Comp Physiol A 155: 239–247

Staudacher E, Schildberger K (1998) Gating of sensory responses of descending brain neurones during walking in crickets. J Exp Biol 201: 559–572

Warzecha A-K, Egelhaaf M (1996) Intrinsic properties of biological movement detectors prevent the optomotor control system from getting unstable. Philos Trans R Soc Lond B 351: 1579–1591

Warzecha A-K, Egelhaaf M (1997) How reliably does a neuron in the visual motion pathway of the fly encode behaviourally relevant information? Eur J Neurosci 9: 1365–1374

Warzecha A-K, Egelhaaf M, Borst A (1993) Neural circuit tuning fly visual interneurons to motion of small objects. I. Dissection of the circuit by pharmacological and photoinactivation techniques. J Neurophysiol 69: 329–339

Wilson MA, McNaughton B (1993) Dynamics of the hippocampal ensemble code for space. Science 261: 1055–1058

Wolf H, Pearson KG (1987) Intracellular recordings from interneurons and motoneurons in intact flying locusts. J Neurosci Method 21: 345–354

Zeil J, Zanker JM (1997) A glimpse into crabworld. Vision Res 37: 3417–3426